




Bioaccumulation processes for mercury removal from saline waters by green, brown and red living marine macroalgae

Elaine Fabre¹ · Mariana Dias² · Bruno Henriques³ · Thainara Viana² · Nicole Ferreira² · José Soares² · João Pinto² · Carlos Vale⁴ · José Pinheiro-Torres⁵ · Carlos M. Silva⁶ · Eduarda Pereira⁷ 

Received: 7 September 2020 / Accepted: 25 January 2021 / Published online: 14 February 2021
© The Author(s), under exclusive licence to Springer-Verlag GmbH, DE part of Springer Nature 2021

Abstract

Mercury is a very toxic metal that persists and accumulates in the living organisms present in the aquatic systems and its elimination is an urgent need. Two green (*Ulva intestinalis* and *Ulva lactuca*), brown (*Fucus spiralis* and *Fucus vesiculosus*), and red (*Gracilaria* sp. and *Osmundea pinnatifida*) marine macroalgae were tested for mercury removal from saline waters. The ability of each species was evaluated to the initial mercury concentrations of 50, 200, and 500 $\mu\text{g dm}^{-3}$ along 72 h. In general, all species exhibited good performances, removing 80.9–99.9% from solutions with 50 $\mu\text{g dm}^{-3}$, 79.3–98.6% from solutions with 200 $\mu\text{g dm}^{-3}$, and 69.8–97.7% from solutions containing 500 $\mu\text{g dm}^{-3}$ of mercury. Among the macroalgae, *Ulva intestinalis* showed the highest affinity to mercury and it presented an uptake ability up to 1888 $\mu\text{g g}^{-1}$ of Hg(II) and bioconcentration factors up to 3823, which proved its promising potential on Hg removal.

Keywords Bioaccumulation · Mercury · Macroalgae · Affinity · Uptake · Water treatment

Introduction

Bioremediation technologies emerged as promising alternatives for the treatment of contaminated waters. Biosorption and bioaccumulation are the major processes related to the uptake of a sorbate by a sorbent of biological origin (Farooq

et al. 2010; Fomina and Gadd 2014; Fabre et al. 2020). If the sorbent is biomass metabolically inactive, the sorption and desorption occur on its surface until equilibrium is achieved (Chung et al. 2007). In the case of a living organism, sorption may be followed by the metabolically active transport systems into the cells (Chojnacka 2010). The transport of the sorbate to the inside of cells makes available more active sites on sorbent surface and, hence, final concentrations in solution may be lower (Chojnacka 2010; Aryal and Liakopoulou-Kyriakides 2015). The limitations of these processes with living organisms are their resistance and adaptation to contaminants. Major environmental factors are those affecting biological processes, such as light exposure, temperature, pH, and nutrient sources (Chojnacka 2010). In the point of view of cost-effective application, the use of living organisms eliminates the step of biomass separation usually required in biosorption with non-living biomass. Moreover, it reduces expenses with other operations such as drying, milling, and storage (Aksu and Dönmez 2005; Chojnacka 2010). Among the living organisms, macroalgae are pointed out as very resistant to extremely polluted medium and capable of retaining high concentrations of metals (Kumar et al. 2006; Chojnacka 2010). Along their natural processes of nutrients uptake, contaminants may be removed from the medium. Examples of species tested as biosorbents are *Enteromorpha* sp. for Cr removal

Responsible Editor: Vitor Manuel Oliveira Vasconcelos

✉ Carlos M. Silva
carlos.manuel@ua.pt

✉ Eduarda Pereira
eduper@ua.pt

- ¹ CICECO & CESAM, Department of Chemistry, University of Aveiro, Aveiro, Portugal
- ² Department of Chemistry, University of Aveiro, Aveiro, Portugal
- ³ CESAM & LAQV-REQUIMTE, Department of Chemistry, University of Aveiro, Aveiro, Portugal
- ⁴ CIIMAR, University of Porto, Matosinhos, Portugal
- ⁵ N9Ve, Nature, Ocean, and Value, Lda., Porto, Portugal
- ⁶ CICECO, Department of Chemistry, University of Aveiro, Aveiro, Portugal
- ⁷ LAQV-REQUIMTE, Department of Chemistry, University of Aveiro, Aveiro, Portugal

(Rangabhashiyam et al. 2016), *Zygnema fanicum* (Shams Khoramabadi et al. 2008), *Cystoseira baccata* (Herrero et al. 2005), and *Porphyridium cruentum* (Zaib et al. 2016) for Hg and *Fucus vesiculosus* for Cd (Holan et al. 1993), Ni and Pb (Holan and Volesky 1994).

Macroalgae are commonly divided in three groups: Chlorophyta (green algae), Phaeophyta (brown algae), and Rhodophyta (red algae) (Bold and Wynne 1978). Although sharing common characteristic of containing chlorophyll, remarkable differences are noticed in pigmentation and composition of cell walls. The Chlorophyta pigments are chlorophylls, carotenes, and xanthophylls; the Phaeophyta have in addition fucoxanthin, while the pigmentation of Rhodophyta is due to the chlorophylls, phycocyanins, phycoerythrins, carotenes, and xanthophylls. The cell walls of all macroalgae are composed of cellulose. In addition, the green macroalgae cell walls have mannan and xylan, the brown macroalgae have alginic acid and fucoidan and the red macroalgae are formed by xylans and galactans. These compounds are formed by amine, carboxyl, sulfates, and hydroxyl, with high tendency to bind with metals in solution (Bold and Wynne 1978; Bulgariu and Bulgariu 2012; He and Chen 2014).

Mercury is the third most toxic element according to the list of priority pollutants created by the Agency for Toxic Substances and Disease Registry (ATSDR) (ATSDR 2015). Such position is attributed to its high frequency and persistence in the environment and its hazardous impacts on the ecosystem and human health (Yavuz et al. 2006; Fabre et al. 2020). Mercury forms are rapidly absorbed by organisms and slower eliminated, being transmitted and magnified along the food chain (Huang et al. 2015). Trace Hg(II) concentrations in water are considered to represent dangerousness, and therefore, contaminated wastewaters must be remediated (Gupta et al. 2004; Fabre et al. 2019). In saline waters, Hg concentration may achieve concentration levels of $27 \mu\text{g dm}^{-3}$ in the Mediterranean Sea (Tunisia) (Nasfi 1995) or $2 \mu\text{g dm}^{-3}$ in the Red Sea (Gworek et al. 2016). However, due to the accumulation of Hg emissions in the aquatic environment along the years, it is expected that these concentrations will rise to much higher levels. For instance, Sunderland et al. (2009) have demonstrated that Hg concentrations in the North Pacific Ocean may increase 50% until 2050 (Sunderland et al. 2009).

In line with the present scientific knowledge, the European Union promotes the improvement of surface water quality by reducing the discharges of priority hazardous substances like Hg(II), and by the development of new technologies more economic and effective to treat contaminated waters (European Commission 2013).

Accordingly, the present study aims to evaluate and compare the ability of *Ulva intestinalis*, *Ulva lactuca*, *Fucus spiralis*, *Fucus vesiculosus*, *Gracilaria* sp., and *Osmundea pinnatifida* for the removal of Hg(II) from contaminated saline waters, in order to offer a potential alternative for water

treatments and reduce the impacts caused by the discharges of this contaminant. The use of saline waters does not only limit the application of these macroalgae only for aquatic systems but also promote the evaluation of their performance under high ionic strength condition which is characteristic of many industrial effluents. Among the large diversity of marine macroalgae, these species were considered for this work due to their abundance in Portugal's coast and presence around the world. The macroalgae species were characterized and their removal efficiencies were examined. Kinetic studies were performed and fitting of pseudo-first-order, pseudo-second-order, and Elovich models to the experimental data were considered.

Materials and methods

Chemicals

The reagents used in this work were purchased by chemical suppliers: mercury(II) nitrate stock solution ($1000 \pm 2 \text{ mg dm}^{-3}$) from PanReac AppliChem and nitric acid (65 %) and sodium hydroxide ($\geq 99 \%$) from Merck. The salt used to prepare the saline solutions was tropic Marin® SEA SALT acquired from Tropic Marine Center. This salt is a complex mixture of minerals that has been used in many toxicological studies due to its composition that faithfully reproduces the characteristics of seawater (Leverett and Thain 2013). The complete information about the salt composition is given by Atkinson and Bingman (2010). The working solutions and the standards for calibration curves were prepared by diluting the stock solution to the desired concentration. All the glassware used in this work were earlier washed with nitric acid (25 %, v/v) for at least 24 h and ultrapure water ($18 \text{ M}\Omega \text{ cm}^{-1}$) afterwards.

Macroalgae

Six macroalgae species were used in this study, two green (*U. lactuca*, *U. intestinalis*), two brown (*F. spiralis*, *F. vesiculosus*), and two red (*Gracilaria* sp., *O. pinnatifida*) macroalgae. Samples were collected from Ria de Aveiro, Portugal ($40^\circ 38' 39'' \text{ N}$, $8^\circ 44' 43'' \text{ W}$), and the species identification was conducted at the Biology Department of the University of Aveiro, based on physical and morphological characteristics. The macroalgae selected for this study are the most abundant species in Aveiro estuary, whose population distribution and identification are well characterized in several theses and published works (Coelho et al. 2005; Abreu et al. 2011; Gonçalves et al. 2019). For that reason, no voucher specimen was deposited in the local publicly available herbarium. At laboratory, macroalgae were washed with tap water and synthetic seawater several times to eliminate some impurities or epibionts imbed on the macroalgae surface. Then, the

macroalgae were maintained in oxygenated aquaria with natural light exposure (about 12L:12D) for acclimation during 1 week before the experiments start. Ten samples of each macroalga were weighted and dried for the determination of water content. Another portion of each macroalga was lyophilized for further quantification of Hg initial concentration and FTIR analysis.

Experiments

All the macroalgae were investigated for Hg(II) removal in 1 dm³ transparent glass flasks and temperature of 22 ± 2 °C. Synthetic seawater of salinity 30 g dm⁻³ was prepared diluting tropic Marin® SEA SALT in distilled water. The macroalgae were cut into small pieces and introduced into the flasks. The dosage of 3 g dm⁻³ (fresh weight) of each species was put in contact with Hg(II) solutions of 50 µg dm⁻³, 200 µg dm⁻³, and 500 µg dm⁻³. The pH was adjusted to 8.5 with NaOH (1 M). Two assays of each condition (macroalgae species and initial concentration) were carried out together with control solutions (without macroalgae) with the aim to verify the experimental losses, and with blank solutions (without Hg(II)) to check the macroalgae health status. The results presented in this study correspond to one of the assays, because the variation in each pair of assays remained below 10%. Liquid samples of 10 cm³ were taken after 0, 1, 3, 6, 9, 24, 48, and 72 h, acidified with nitric acid (65%, v/v) for pH ≤ 2 and stored at 4°C for further Hg(II) quantification. The volume variation due to sampling was insufficient to significantly affect the results. In the end of each assay, the macroalgae were removed from the solution, weighted to quantify the relative growth rate, lyophilized, and stored for FTIR characterization.

Hg(II) quantification

Mercury quantification in solution was performed by cold vapor atomic fluorescence spectroscopy (CV-AFS), on a PSA cold vapor generator (model 10.003) connected to a Merlin PSA detector (model 10.023). Hg(II) in the samples was reduced by SnCl₂ and the response was obtained as signal converted to concentration through a calibration curve, constructed at least three times a day with the standards of 0.1, 0.2, 0.3, and 0.5 µg dm⁻³ of Hg(II). Three measures of each sample were performed with a maximum acceptable variation of 10% between them and the average value was used. The limit of quantification of this method was 0.02 µg dm⁻³.

The concentration of Hg(II) in the macroalgae before the bioaccumulation assays was quantified using LECO® AMA-254 by thermal decomposition atomic absorption spectrometry with gold amalgamation according to the method reported by Costley et al. (2000). The limit of quantification was 0.03 ng of Hg. Samples were analyzed in triplicate with variation coefficients between concentrations lower than 10%.

The Certified Reference Material (CRM) ERM-CD200 (*Fucus vesiculosus*; 0.0186 ± 0.0016 mg kg⁻¹ of total Hg) was analyzed before and after the macroalgae samples to assure the quality of the results obtained. The average percentage of recovery was 100.8%.

Macroalgae characterization

The six macroalgae species studied were characterized by water content, external contact area, and FTIR. The water content was accounted for by weighing ten samples of each macroalgae before and after drying. External contact area was assessed by scanning fixed masses of the macroalgae with resolution of 200 ppi and the software Fiji scaled the image. Fourier transform infrared (FTIR) spectra of the macroalgae before and after contact with the contaminated solutions were recorded by Bruker optic tensor 27 spectrometer with an attenuated total reflectance (ATR), 256 scans with a resolution of 4 cm⁻¹. Samples were directly analyzed and spectra were obtained after baseline correction from the wavenumber 4000 to 500 cm⁻¹.

Formula and data analysis

The removal of Hg(II) by the macroalgae (R, %) was calculated by the following equation:

$$R = 100 \times \frac{(C_{A0} - C_A)}{C_{A0}} \tag{1}$$

where C_{A0} (µg dm⁻³) is the initial Hg(II) concentration in the spiked solutions and C_A (µg dm⁻³) the concentration at time *t*.

The mass balance of each experiment allows to calculate the average Hg(II) concentration per mass of dry weight of macroalgae (q_A, µg g⁻¹) at time *t* as follows:

$$q_A = \frac{V(C_{A0} - C_A)}{M} \tag{2}$$

where *V* is the volume of solution in dm³ and *M* is the average mass between initial and final weights in dry weight (g).

Assuming an exponential growth of the macroalgae, the relative growth rate (RGR, % day⁻¹) of the experiment was mathematically expressed by (Gordillo et al. 2015):

$$RGR = 100 \times \frac{\ln(W_f/W_0)}{t} \tag{3}$$

where W₀ is the initial fresh weight (g) of the macroalgae and W_f is the weight after 72 h of exposure to Hg(II) contaminated solutions; *t* is the time of the experiment, 72 h expressed in days.

The bioconcentration factor (BCF) was calculated by:

$$BCF = 1000 \times \frac{q_A}{C_{A0}} \quad (4)$$

where q_A ($\mu\text{g g}^{-1}$) is the macroalgae concentration obtained from Eq. (2) at a time of 72 h and C_{A0} is the Hg(II) initial concentration in $\mu\text{g kg}^{-1}$ (assuming that 1 dm^3 of the solution is equal to 1 kg).

The kinetic study was accomplished by fitting the most known kinetic models of pseudo-first-order (Eq. (5)) (Lagergren 1898), pseudo-second-order (Eq. (6)) (Ho and McKay 1999), and Elovich (Eq. (7)) (Roginsky and Zeldovich 1934) to the experimental results. These models give information about the viability of the application of the process, taking into account the velocity and affinity of the macroalgae for Hg(II) bioaccumulation.

$$\frac{dq_A}{dt} = k_1(q_{Ac} - q_A) \quad (5)$$

$$\frac{dq_A}{dt} = k_2(q_{Ac} - q_A)^2 \quad (6)$$

$$\frac{dq_A}{dt} = \alpha e^{-\beta q_A} \quad (7)$$

where q_{Ac} is the concentration on the macroalgae at equilibrium ($\mu\text{g g}^{-1}$), k_1 (h^{-1}) is the rate constant of the pseudo-first-order model, k_2 ($\text{g } \mu\text{g}^{-1} \text{ h}^{-1}$) is the rate constant of the pseudo-second-order model, α ($\mu\text{g g}^{-1} \text{ h}^{-1}$) is the initial sorption rate, and β ($\text{g } \mu\text{g}^{-1}$) is the desorption constant.

The parameters of the models were obtained by non-linear optimization using the software Matlab R2014a in which the errors between experimental and calculated data (AARD, Eq. (8)) were minimized by the Nelder-Mead simplex algorithm. The goodness of the fits was evaluated by the average absolute relative deviation, AARD (Eq. (8)), and the coefficient of determination, R^2 (Eq. (9)) represented by:

$$AARD(\%) = \frac{100}{N_{DP}} \sum_{i=1}^{N_{DP}} \frac{|\hat{y}_i - y_i|}{y_i} \quad (8)$$

$$R^2 = 1 - \frac{\sum (\hat{y}_i - y_i)^2}{\sum (y_i - \bar{y})^2} \quad (9)$$

N_{DP} denotes the number of experimental data, y_i , and \hat{y}_i represent the observed and calculated values, and \bar{y} is the mean of experimental data.

Significance tests were done by one-way analysis of variance (ANOVA) test, with a confidence interval of 95 %, using the data analysis extension of Microsoft® Excel™ 2016.

Results and discussion

Major characteristics of macroalgae

Water content (%), contact external area, and initial concentration of Hg(II) of the macroalgae used in the experiments are presented in Table 1. Regarding water content, the six macroalgae can be separated into two groups, presenting statistical dissimilarities ($p < 0.05$): group I includes *U. intestinalis*, *Gracilaria* sp. and *O. pinnatifida*; and group II contains *U. lactuca*, *F. spiralis*, and *F. vesiculosus*. *U. intestinalis* showed the highest water content (91%) and *F. vesiculosus* the lowest (80%). Contact external areas of the green macroalgae stand out due to their morphologies like thin leaves with round or tubular shapes. Brown macroalgae have branched shapes with alginic pouches which make them denser. The red macroalgae *Gracilaria* sp. have filamentous shapes and thin branches, and *O. pinnatifida* has branched stems and flattened fronds. Although Hg(II) initial concentration differed significantly ($p < 0.05$) among the macroalgae species used in the experiments, values were characteristic of low contaminated regions (Coelho et al. 2005; Henriques et al. 2015).

Figure 1 depicts the FTIR spectra of the six macroalgae before and after the exposure assays. Major functional groups involved on the Hg(II) uptake were identified by the appearance, disappearance, or shift of the peaks comparing the spectra of macroalgae before and after exposure to Hg(II) spiked solutions. All the macroalgae presented the O–H and N–H vibrations at 3200–3400 cm^{-1} , the stretch at 2900 cm^{-1} related to the asymmetric C–H bonds, the peak of asymmetric C=O nearby 1600 cm^{-1} , and symmetric C=O around 1400 cm^{-1} . The strong vibration at 1000–1100 is ascribed to the hydroxyl group of the characteristic main sugars present in the macroalgae. In the spectrum of *U. intestinalis*/Hg(II), there is the appearance of the peak at 1536 cm^{-1} correspondent to N–H of amide II groups of proteins (Murphy et al. 2009; Rodrigues et al. 2015), the formation of a double peak at 2910 and 2980 cm^{-1} of the C–H (Rodrigues et al. 2015), and the vanishing of the elbow at 1318 cm^{-1} of sulfonate groups (-OSO₃) (Murphy et al. 2009). In the case of *U. lactuca*, after contact with the Hg(II) solution, there is the formation of a double peak at 2910 and 2990 cm^{-1} (C–H) (Rodrigues et al. 2015), elimination of the band at 1120 cm^{-1} (symmetric-OSO₃) (Murphy et al. 2009), shift of the peaks at 1090 and 1010 cm^{-1} due to the involvement of the hydroxyl functional groups (Murphy et al. 2008), and shift at 1197 cm^{-1} assigned to the C–N stretching of the aromatic amine (Suganya and Renganathan 2012). *F. spiralis*/Hg(II) and *F. vesiculosus*/Hg(II) spectra were very similar. The elimination of the double at 2850–2920 cm^{-1} (C–H) (Rodrigues et al. 2015) and disappearance of the vibrations at 1540 cm^{-1} (N–H) (Murphy et al. 2009) and 550 cm^{-1} (C–N–S) (Bulgariu and

Table 1 Water content (%), external area of contact (cm² g⁻¹), and Hg concentration (μg g⁻¹) of the living macroalgae used in the experiments

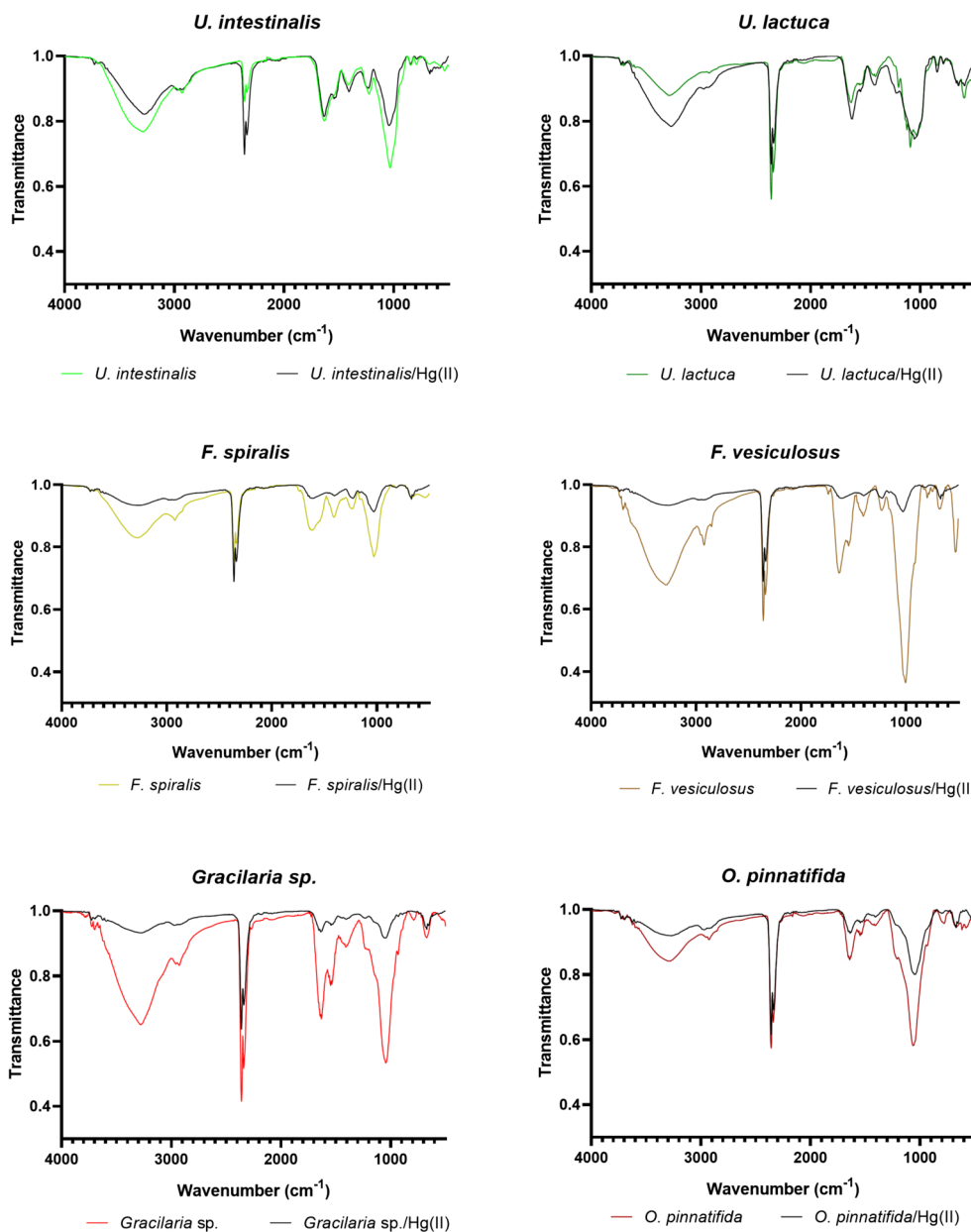
	Macroalgae					
	<i>Ulva intestinalis</i>	<i>Ulva lactuca</i>	<i>Fucus spiralis</i>	<i>Fucus vesiculosus</i>	<i>Gracilaria</i> sp.	<i>Osmundea pinnatifida</i>
Water content (%)	91.4 ± 0.6	82.8 ± 0.5	81.6 ± 3.1	80.2 ± 5.4	88.1 ± 5.5	88.8 ± 1.2
External contact area (cm ² g ⁻¹)	148 ± 45	264 ± 31	29 ± 11	30 ± 9	79 ± 9	33 ± 2
Hg concentration (μg g ⁻¹)	0.042 ± 0.002	0.034 ± 0.002	0.049 ± 0.002	0.032 ± 0.001	0.031 ± 0.002	0.082 ± 0.002

Bulgariu 2014) were noticed. Regarding the red macroalgae spectra, both presented the vanishing of the band at 800 cm⁻¹ (-OSO₃) attributed to the galactose contained in carrageenan (Knutsen et al. 1994; Rodrigues et al. 2015). *Gracilaria* sp.

exposed to Hg(II) showed the shift of the peak at 1110 cm⁻¹ (O–H) assigned to the presence of agar.

Relative growth rates (RGR) of the macroalgae during the 72 h of the experiments were calculated by Eq. (3) and values

Fig. 1 FTIR spectra of the six macroalgae before and after Hg(II) exposure



are given in Table 2. *RGR* varied with narrow intervals in species exposed to $50 \mu\text{g dm}^{-3}$ (-1.2 to $3.2\% \text{ day}^{-1}$) and $200 \mu\text{g dm}^{-3}$ (-2.2 to $0.5\% \text{ day}^{-1}$). Exposure to $500 \mu\text{g dm}^{-3}$ resulted in broader variation of weight, *RGR* varying from $-11.7\% \text{ day}^{-1}$ for *O. pinnatifida* to $3.2\% \text{ day}^{-1}$ for *U. lactuca*. The negative values of relative growth rates were probably associated with some losses in the recovery of the macroalgae or loss of weight due to stress caused by the contaminated medium as it was verified by marked loss of color and deterioration in the end of the trial in the case of *O. pinnatifida*, exposed to the Hg(II) concentration of $500 \mu\text{g dm}^{-3}$. Positive values of *RGR* may represent higher uptake ability due to new available sorption sites on the macroalgae surface.

Influence of Hg(II) initial concentrations on removal

Figure 2 shows the Hg(II) concentrations in solution at each time (C_A), normalized to the initial concentration (C_{A0}), along 72 h, for the six macroalgae. The profiles for the initial concentrations of 50 , 200 , and $500 \mu\text{g dm}^{-3}$ are presented. Although the results of control experiments are not shown, they remained stable and the variation in Hg concentration was lower than 5% . For all the conditions, ratios $C_A : C_{A0}$ decreased with time. Although slopes varied with the macroalgae species, only small differences were observed among the three spiking conditions. All the curves of *U. intestinalis* and the curves of *U. lactuca* and *Gracilaria* sp. for 50 and $500 \mu\text{g dm}^{-3}$ were remarkably characterized by slopes with two stages: the first one shows a pronounced slope, the fast removal being driven by the strong gradient of Hg between the solution and the clean macroalgae; in the second stage, the removal slowed down towards an equilibrium. Change in removal rates may be associated with two dynamics of Hg(II) uptake: initially, Hg was extracellularly bound to the macroalgae by chemical or physical interactions, and then by intracellular accumulation driven by metabolic activities, which are normally slower than sorption (Kadukova and Vireikova 2005; Andrade et al. 2006; Henriques et al. 2015). In the profiles observed for the other studied species, the two stages were less pronounced. Decrease of C_A/C_{A0} in *F. spiralis*, *F. vesiculosus*, and *O. pinnatifida* was almost linear, which may reflect lower affinity of the freshly arrived Hg cations to functional groups

of the macroalgae surface, or difficult accessibility of Hg(II) to the active sorption sites.

Along time, the differences among the concentration profiles obtained for 50 , 200 , and $500 \mu\text{g dm}^{-3}$ experiments were minor for the macroalgae *U. intestinalis*, *F. spiralis*, *F. vesiculosus*, and *O. pinnatifida*. The low variability suggests that increasing concentration of Hg(II) in solution, and consequently higher fluxes towards the macroalgae surface, led to a proportional uptake, i.e., since more Hg was accumulated by macroalgae in more concentrated solutions. Presumably, the saturation of the sorption sites was not achieved for the tested concentrations. Although all the six macroalgae have achieved low final concentrations of Hg in solution, *U. intestinalis* appears as the most promising macroalgae.

Figure 3 shows the removal percentages by the six macroalgae (3 g dm^{-3}) for the three initial Hg(II) concentrations. After 72 h of contact with the spiked solution of $50 \mu\text{g dm}^{-3}$, *Gracilaria* sp., *U. lactuca*, and *U. intestinalis* removed 99.9% , 99.6% , and 98.2% of Hg(II), respectively, and their final solutions have achieved concentrations of drinking water quality regulation ($< 1 \mu\text{g dm}^{-3}$) (Directive 2008/105/EC 2008). *U. intestinalis* showed the best performance in the conditions of exposure to concentrations of 200 and $500 \mu\text{g dm}^{-3}$, with Hg(II) removal of 98.6% and 97.3% , respectively. These results are reflective of the absence of restrictions for mercury removal by *U. intestinalis*, and it is intuitive that if higher Hg(II) concentrations were tested, low residual concentrations in solution would be observed. The worst accomplishments were those of *O. pinnatifida* (80.9%) under the initial concentration of $50 \mu\text{g dm}^{-3}$, *F. vesiculosus* (79.3%) under $200 \mu\text{g dm}^{-3}$, and *O. pinnatifida* (69.8%) under $500 \mu\text{g dm}^{-3}$. Due to the mass loss of *O. pinnatifida* observed after 72 h in contact with the most contaminated solution (negative *RGR*), it should not be excluded the possibility of low removal being a consequence of toxicity effect.

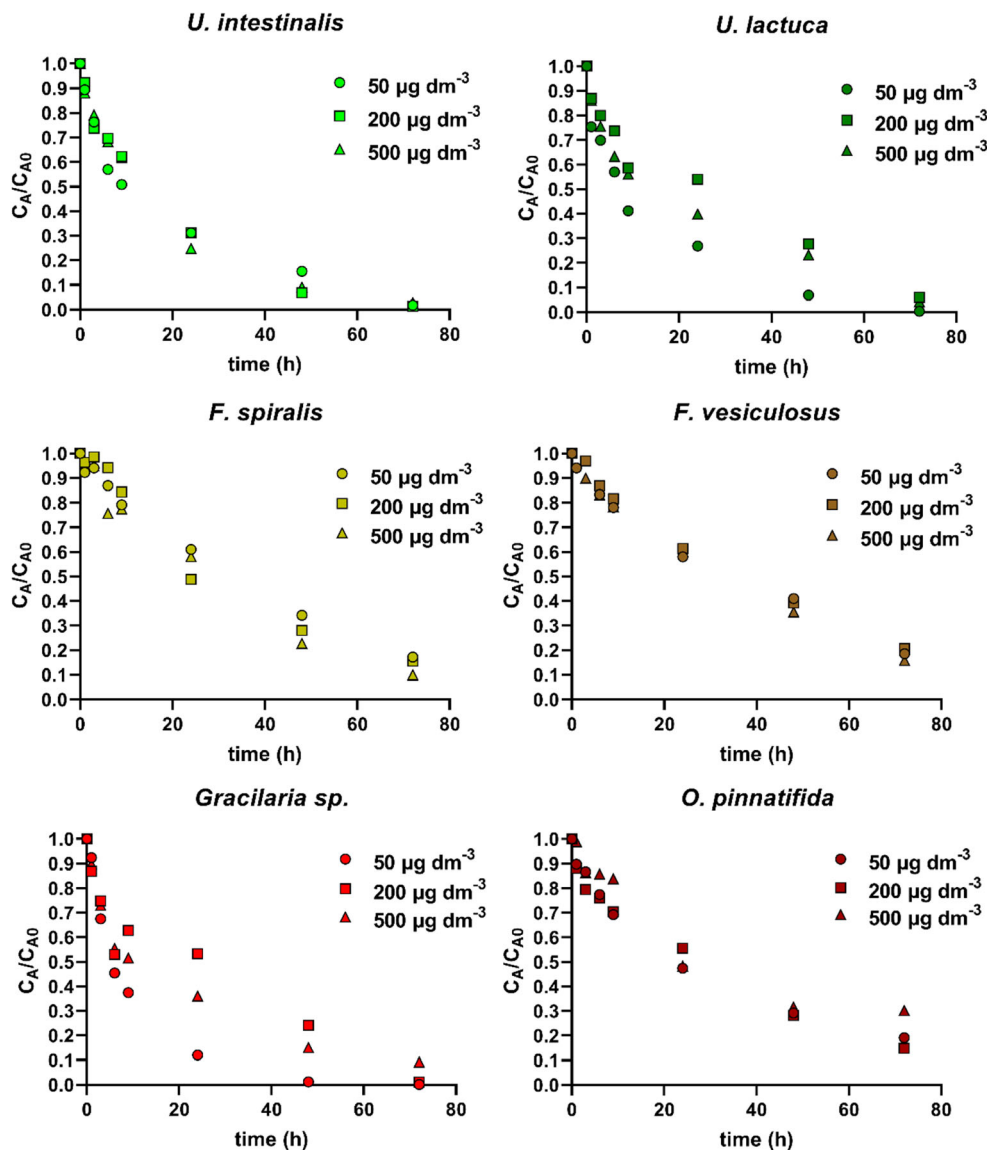
Uptake of Hg(II) by macroalgae

Figure 4 presents the calculated mass of Hg uptake (q_A) by the green, brown, and red macroalgae in dry weight (Eq. (2)) along time for the three initial concentrations. In line with the normalized concentration profiles, *U. intestinalis* showed

Table 2 Relative growth rates (*RGR*, % day^{-1}) of the macroalgae during the 72 h calculated by Eq. (3)

<i>RGR</i> (% day^{-1})	<i>Ulva intestinalis</i>	<i>Ulva lactuca</i>	<i>Fucus spiralis</i>	<i>Fucus vesiculosus</i>	<i>Gracilaria</i> sp.	<i>Osmundea pinnatifida</i>
$50 \mu\text{g dm}^{-3}$	0.6	3.2	- 0.3	- 0.6	1.1	- 1.2
$200 \mu\text{g dm}^{-3}$	0.5	0.5	- 1.7	- 0.5	- 0.7	- 2.2
$500 \mu\text{g dm}^{-3}$	3.1	3.2	- 1.6	- 0.04	- 4.5	- 11.7

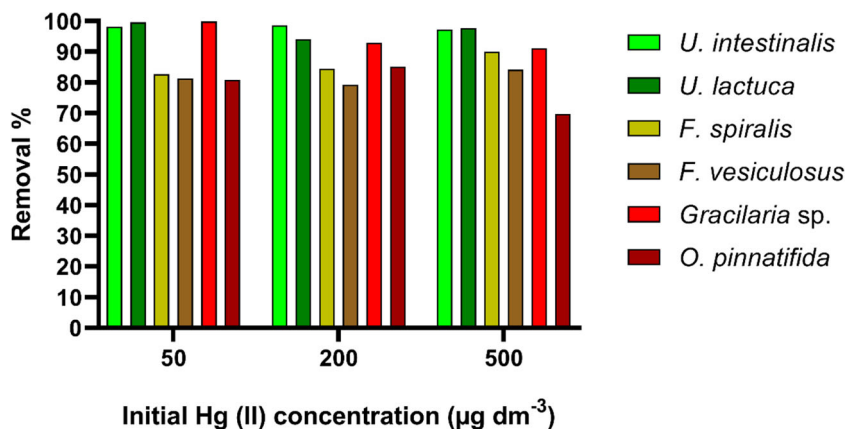
Fig. 2 Normalized Hg(II) concentration of the solution along time for three different initial concentrations and six macroalgae



the highest uptake for all the studied conditions. Since the same mass of macroalgae in fresh weight was used in the experiments, *U. intestinalis* presented the lowest mass (in

dry weight) used in the experiments in comparison with the other macroalgae, such as *U. lactuca* that presented lower water content and therefore larger doses. Besides that,

Fig. 3 Removal percentages of Hg(II) from contaminated solutions with 50, 200, and 500 $\mu\text{g dm}^{-3}$ for all the macroalgae studied after 72 h of contact time



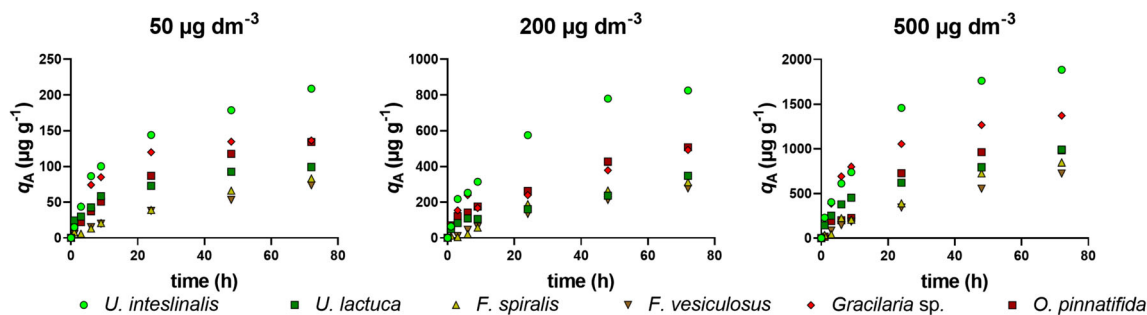


Fig. 4 Hg(II) concentration on the macroalgae along time for the three different scenarios of contamination

U. intestinalis exhibited high external contact area and its thin tubular structure may facilitate the removal of cations from the solution. For the two lower Hg concentrations, brown and red macroalgae showed similar behaviors, probably as a result of their similar morphology and composition. The plateau observed in the case of *Gracilaria* sp. exposed to $50 \mu\text{g dm}^{-3}$ suggests an almost total removal of Hg(II) after 48 h. It should be considered the possibility of living macroalgae incorporating Hg(II) by carrier proteins through nutrients transport processes, which would make available sorption sites (Stumm and Morgan 1996). Under these conditions, the equilibrium state of the Hg sorption would be repeatedly adjusted and saturation of the sites is not reached (Stumm and Morgan 1996). Higher values of q_A were obtained for higher initial Hg concentrations. For example, in the experiments of $50 \mu\text{g dm}^{-3}$, the quantities of Hg(II) retained in the macroalgae varied from $74 \mu\text{g g}^{-1}$ for *F. vesiculosus* to $209 \mu\text{g g}^{-1}$ for *U. intestinalis*, while for the initial concentration of $500 \mu\text{g dm}^{-3}$ q_A was between $727 \mu\text{g g}^{-1}$ for *F. vesiculosus* and $1888 \mu\text{g g}^{-1}$ for *U. intestinalis*.

Kinetics modeling

The kinetic models of PFO, PSO, and Elovich were fitted to the experimental data of *U. intestinalis*; this macroalga was chosen due to its best performance on the removal of Hg(II). The adjusted curves are plotted in Fig. 5 and the parameters obtained are presented in Table 3. Good

agreements were obtained between the fittings of the models and the experimental data, with coefficients of determination in the range of 0.971–0.991 for PFO, 0.987–0.990 for PSO, and 0.986–0.989 for Elovich models. Globally, PSO and Elovich equations presented the best combinations of higher values of R^2 and lower AARD and, consequently, are better for the description of Hg(II) kinetics by *U. intestinalis*. The constant of the PSO model k_2 decreased with the higher concentrations. This parameter is related to the time to reach the equilibrium and higher values represent shorter equilibrium time (Plazinski et al. 2009). Therefore, less-contaminated solutions tend to get the equilibrium state earlier. However, the initial sorption parameter of the Elovich model α followed the initial concentration pattern, which corroborates with the enhance in the Hg(II) concentration gradient between solution and macroalga surface that promoted higher uptake of Hg(II).

Bioconcentration factor

Table 4 shows the bioconcentration factor (BCF) calculated by Eq. (4) for the six macroalgae exposed for 72 h to solutions with $50, 200, \text{ and } 500 \mu\text{g dm}^{-3}$ of Hg(II). BCFs varied within the broad interval of 1357–3823. The species of macroalgae contributed more to the variation of the BCF than the different contamination in solution. Narrow variation of BCFs for the

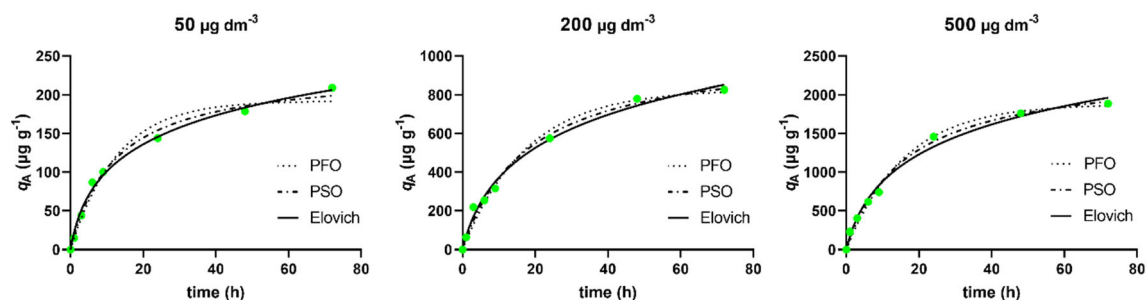


Fig. 5 Kinetic fitting to the experimental data of *U. intestinalis*

Table 3 Kinetic parameters of the models of PFO, PSO, and Elovich models for *U. intestinalis*

Hg(II) initial concentration (µg dm ⁻³)	PFO model				PSO model				Elovich model			
	<i>k</i> ₁ (h ⁻¹)	<i>q</i> _e (µg g ⁻¹)	<i>R</i> ²	AARD (%)	<i>k</i> ₂ (g mg ⁻¹ h ⁻¹)	<i>q</i> _e (µg g ⁻¹)	<i>R</i> ²	AARD (%)	<i>α</i> (µg g ⁻¹ h ⁻¹)	<i>β</i> (g µg ⁻¹)	<i>R</i> ²	AARD (%)
50	0.090	181.2	0.971	5.33	3.602E-04	224.8	0.987	5.36	20.79	0.0151	0.989	6.74
200	0.061	824.4	0.983	10.46	5.330E-05	1040.2	0.989	8.18	73.22	0.0036	0.989	6.03
500	0.068	1833.8	0.991	10.26	3.252E-05	2246.8	0.990	8.55	193.48	0.0017	0.986	7.38

three contamination conditions might be ascribed to the chemical equilibrium of Hg(II) between solution and macroalgae surface. This is a remarkable result because it emphasizes the high capacity of the studied macroalgae to store Hg, at least until the presence of 500 µg dm⁻³ in solution. *U. intestinalis* was much more efficient to concentrate Hg(II) than the other macroalgae, and brown and red macroalgae presented similar BCFs (*p* > 0.05). In terms of practical aspects, these outcomes are very promising, since even the species that performed worst were able to accumulate mercury three orders of magnitude above than the contaminated medium.

Comparison with different sorbents from literature

The removal efficiencies of the six macroalgae tested in this work have been compared with different sorbents used to remove Hg(II) in similar initial concentrations (50 and 500 µg dm⁻³) and the results are displayed in Table 5. It is possible to observe that small doses of macroalgae as low as the ones used in this study were able to perform equally or even better than the sorbents reported in the literature. *Gracilaria* sp. presented the same performance of the magnetic nanoparticles Fe₃O₄@SiO₂/SiDTC in similar matrices and spiked Hg(II) concentration of 50 µg dm⁻³ and its use allows to

obtain a decontaminated solution. All the other biosorbents and synthetic materials showed worse performances than *Gracilaria* sp. under this Hg(II) concentration, even the materials tested were under simpler water matrices. Comparing the performances of the macroalgae under the highest Hg(II) initial concentration studied, *U. lactuca* presented better removal percentage than the biosorbents rice husks, cork stoppers, crab carapace, and clamshell wastes.

It is worth mentioning that these materials may have associated costs of synthetization and/or separation at the end of the process. In the case of bioaccumulation using the macroalgae considered in this study, the additional steps of filtration and biosorbent storage and pre-treatment are dismissed and the process becomes more viable and attractive. Comparison with other materials highlighted the potential of using this sustainable bioremediation process using living macroalgae in alternative to other sorbents for water treatment.

Conclusions

The performances of the macroalgae to uptake Hg from solutions followed the sequence green > red > brown. Uptake increased with time and with initial mercury concentration, although without reach a plateau. This pattern is indicative of a lack of saturation of the active binding sites on the macroalgae surface, probably due to Hg bioaccumulation in the inner part of the macroalgae cells by active means. However, this study does not allow to distinguish mercury uptake through physical-chemical interactions at macroalgae surface and incorporation by metabolic activities. High bioconcentration factors of the macroalgae for the three spiking conditions, in particular *U. intestinalis*, point to the excellent performance of these species on mercury removal. In addition, the comparison with different materials reported in the literature highlighted the potential of using this simple sustainable and efficient alternative for the treatment of contaminated waters.

Table 4 Bioconcentration factor (BCF) of the macroalgae for the contaminated solutions with 50, 200, and 500 µg dm⁻³ of Hg(II)

Macroalgae	Bioconcentration factor (BCF)		
	50 µg dm ⁻³	200 µg dm ⁻³	500 µg dm ⁻³
<i>U. intestinalis</i>	3803	3823	3773
<i>U. lactuca</i>	1953	1738	1877
<i>F. spiralis</i>	1500	1531	1630
<i>F. vesiculosus</i>	1357	1321	1404
<i>Gracilaria</i> sp.	2775	2462	2574
<i>O. pinnatifida</i>	2450	2581	2115

Table 5 Comparison of the Hg(II) removal efficiencies for different materials

Sorbent	Type of water matrix	Hg(II) initial concentration ($\mu\text{g dm}^{-3}$)	Sorbent dosage (g dm^{-3})	Time of exposure (h)	Removal (%)	Ref.
<i>U. intestinalis</i>	Synthetic seawater	50	0.26	72	98.2	This study
<i>U. lactuca</i>	Synthetic seawater	50	0.52	72	99.6	This study
<i>F. spiralis</i>	Synthetic seawater	50	0.55	72	82.8	This study
<i>F. vesiculosus</i>	Synthetic seawater	50	0.59	72	81.4	This study
<i>Gracilaria</i> sp.	Synthetic seawater	50	0.36	72	99.9	This study
<i>O. pinnatifida</i>	Synthetic seawater	50	0.34	72	80.9	This study
Rice husks	Ultrapure	50	0.25	168	82.0	Rocha et al. (2013)
Rice husks	Ultrapure	50	0.50	168	84.0	Rocha et al. (2013)
Cork stoppers	seawater	50	0.25	96	48.0	Lopes et al. (2014)
Crab carapace	Ultrapure	50	0.25	72	62.0	Monteiro et al. (2016)
Clam shell wastes	Ultrapure	50	0.25	72	80.0	Monteiro et al. (2016)
Graphene oxide	Seawater	50	0.01	48	42.0	Henriques et al. (2016)
$\text{Fe}_3\text{O}_4@\text{SiO}_2/\text{SiDTC}$	Seawater	50	0.01	48	99.9	Tavares et al. (2016)
ETS-4	Ultrapure	50	0.016	24	99.5	Lopes et al. (2009)
<i>U. intestinalis</i>	Synthetic seawater	500	0.26	72	97.3	This study
<i>U. lactuca</i>	Synthetic seawater	500	0.52	72	97.7	This study
<i>F. spiralis</i>	Synthetic seawater	500	0.55	72	90.0	This study
<i>F. vesiculosus</i>	Synthetic seawater	500	0.59	72	84.2	This study
<i>Gracilaria</i> sp.	Synthetic seawater	500	0.36	72	91.1	This study
<i>O. pinnatifida</i>	Synthetic seawater	500	0.34	72	69.8	This study
Rice husks	Ultrapure	500	0.25	168	91.0	Rocha et al. (2013)
Rice husks	Ultrapure	500	0.50	168	92.0	Rocha et al. (2013)
Cork stoppers	Ultrapure	500	0.25	168	94.4	Lopes et al. (2014)
Crab carapace	Ultrapure	500	0.25	72	62.0	Monteiro et al. (2016)
Clamshell wastes	Ultrapure	500	0.25	72	83.0	Monteiro et al. (2016)

Data and materials availability All data generated or analyzed during this study are included in this published article (and its supplementary information files) or are available from the corresponding author on reasonable request.

Authors' contribution The authors' contribution to the development of this work is described below:

Elaine Fabre: writing, experimental performing, and data analysis
 Mariana Dias: experimental performing and data analysis
 Bruno Henriques: scientific orientation, data analysis, and writing
 Thainara Viana: experimental performing
 Nicole Ferreira: experimental performing
 José Soares: experimental performing
 João Pinto: experimental performing
 Carlos Vale: scientific orientation, data analysis, and writing
 José M. P. Torres: data analysis and funding acquisition
 Carlos M. Silva: scientific orientation, data analysis, funding acquisition, and writing
 Eduarda Pereira: scientific orientation, data analysis, funding acquisition, and writing

Funding This work has been supported by the project N°46998_N9ve-REE co-funded by Portugal 2020 program (PT2020), PO Centro, and European Structural and Investment Funds. E. Fabre

acknowledges the financial support of CNPq (Conselho Nacional de Desenvolvimento Científico e Tecnológico), Brazil. Bruno Henriques benefited from a Research contract (CEECIND/03511/2018) under the CEEC Individual 2018, funded by national funds (OE), through FCT – Fundação para a Ciência e a Tecnologia, I.P. Thanks are also due to the financial support to CICECO-Aveiro Institute of Materials (UID/CTM/50011/2019) and to CESAM (UID/AMB/50017), by FCT/MEC through national funds, and the co-funding by the FEDER, within the PT2020 Partnership Agreement and Compete 2020.

Declarations

Ethics approval and consent to participate The authors acknowledge that the submitted manuscript was prepared as described in the Guide for Authors, it follows the Ethics in Publishing Policy, and it is not currently being considered for publication elsewhere.

Consent for publication All authors consent to the publication of the manuscript in Environmental and Science Pollution Research.

Competing interests The authors declare no competing interests.

References

- Abreu MH, Pereira R, Sousa-Pinto I, Yarish C (2011) Ecophysiological studies of the non-indigenous species *Gracilaria vermiculophylla* (Rhodophyta) and its abundance patterns in Ria de Aveiro lagoon, Portugal. *Eur J Phycol* 46:453–464. <https://doi.org/10.1080/09670262.2011.633174>
- Aksu Z, Dönmez G (2005) Combined effects of molasses sucrose and reactive dye on the growth and dye bioaccumulation properties of *Candida tropicalis*. *Process Biochem* 40:2443–2454. <https://doi.org/10.1016/j.procbio.2004.09.013>
- Andrade S, Contreras L, Moffett JW, Correa JA (2006) Kinetics of copper accumulation in *Lessonia nigrescens* (Phaeophyceae) under conditions of environmental oxidative stress. *Aquat Toxicol* 78:398–401. <https://doi.org/10.1016/j.aquatox.2006.04.006>
- Aryal M, Liakopoulou-Kyriakides M (2015) Bioremoval of heavy metals by bacterial biomass. *Environ Monit Assess* 187:4173. <https://doi.org/10.1007/s10661-014-4173-z>
- Atkinson MJ, Bingham C (2010) Elemental composition of commercial sea salts. *J Aquaric Aquat Sci* 8:39–43
- ATSDR (2015) Priority List of Hazardous Substances. <https://www.atsdr.cdc.gov/spl/index.html>. Accessed 16 Jan 2017
- Bold HC, Wynne MJ (1978) Introduction to the algae: structure and reproduction. Prentice Hall, New Jersey
- Bulgariu D, Bulgariu L (2012) Equilibrium and kinetics studies of heavy metal ions biosorption on green algae waste biomass. *Bioresour Technol* 103:489–493. <https://doi.org/10.1016/j.biortech.2011.10.016>
- Bulgariu L, Bulgariu D (2014) Enhancing biosorption characteristics of marine green algae (*Ulva lactuca*) for heavy metals removal by alkaline treatment. *Bioprocess Biotech* 4. <https://doi.org/10.4172/2155-9821.1000146>
- Chojnacka K (2010) Biosorption and bioaccumulation – the prospects for practical applications. *Environ Int* 36:299–307. <https://doi.org/10.1016/j.envint.2009.12.001>
- Chung MK, Tsui MTK, Cheung KC et al (2007) Removal of aqueous phenanthrene by brown seaweed *Sargassum hemiphyllum*: Sorption-kinetic and equilibrium studies. *Sep Purif Technol* 54:355–362. <https://doi.org/10.1016/j.seppur.2006.10.008>
- Coelho JP, Pereira ME, Duarte A, Pardal MA (2005) Macroalgae response to a mercury contamination gradient in a temperate coastal lagoon (Ria de Aveiro, Portugal). *Estuar Coast Shelf Sci* 65:492–500. <https://doi.org/10.1016/j.ecss.2005.06.020>
- Costley CT, Mossop KF, Dean JR et al (2000) Determination of mercury in environmental and biological samples using pyrolysis atomic absorption spectrometry with gold amalgamation. *Anal Chim Acta* 405:179–183. [https://doi.org/10.1016/S0003-2670\(99\)00742-4](https://doi.org/10.1016/S0003-2670(99)00742-4)
- Directive 2008/105/EC (2008) Directive 2008/105/EC of the European Parliament and the Council of 16 December 2008 on environmental quality standards in the field of water policy, amending and subsequently repealing Council Directives 82/176/EEC, 83/513/EEC, 84/156/EEC, 84/491/EEC, 86. 348:84–97
- European Commission (2013) Directive 2013/39/EU of the European Parliament and of the Council of 12 August 2013 amending Directives 2000/60/EC and 2008/105/EC as regards priority substances in the field of water policy. In: Off. J. Eur. Union
- Fabre E, Vale C, Pereira E, Silva CM (2019) Experimental measurement and modeling of Hg(II) removal from aqueous solutions using *Eucalyptus globulus* bark: Effect of pH, salinity and biosorbent dosage. *Int J Mol Sci* 20:5973. <https://doi.org/10.3390/ijms20235973>
- Fabre E, Lopes CB, Vale C et al (2020) Valuation of banana peels as an effective biosorbent for mercury removal under low environmental concentrations. *Sci Total Environ* 709:135883. <https://doi.org/10.1016/j.scitotenv.2019.135883>
- Farooq U, Kozinski JA, Khan MA, Athar M (2010) Biosorption of heavy metal ions using wheat based biosorbents - a review of the recent literature. *Bioresour Technol* 101:5043–5053. <https://doi.org/10.1016/j.biortech.2010.02.030>
- Fomina M, Gadd GM (2014) Biosorption: current perspectives on concept, definition and application. *Bioresour Technol* 160:3–14. <https://doi.org/10.1016/j.biortech.2013.12.102>
- Gonçalves MFM, Vicente TFL, Esteves AC, Alves A (2019) *Neptunomyces aureus* gen. et sp. nov. (Didymosphaeriaceae, Pleosporales) isolated from algae in Ria de Aveiro, Portugal. *Mycospora* 60:31–44. <https://doi.org/10.3897/mycokeys.60.37931>
- Gordillo FJL, Aguilera J, Wiencke C, Jiménez C (2015) Ocean acidification modulates the response of two Arctic kelps to ultraviolet radiation. *J Plant Physiol* 173:41–50. <https://doi.org/10.1016/j.jplph.2014.09.008>
- Gupta RK, Singh RA, Dubey SS (2004) Removal of mercury ions from aqueous solutions by composite of polyaniline with polystyrene. *Sep Purif Technol* 38:225–232. <https://doi.org/10.1016/j.seppur.2003.11.009>
- Gworek B, Bemowska-Kalabun O, Kijeńska M, Wrzosek-Jakubowska J (2016) Mercury in marine and oceanic waters—a review. *Water Air Soil Pollut* 227:1–19. <https://doi.org/10.1007/s11270-016-3060-3>
- He J, Chen JP (2014) A comprehensive review on biosorption of heavy metals by algal biomass: Materials, performances, chemistry, and modeling simulation tools. *Bioresour Technol* 160:67–78. <https://doi.org/10.1016/j.biortech.2014.01.068>
- Henriques B, Rocha LS, Lopes CB et al (2015) Study on bioaccumulation and biosorption of mercury by living marine macroalgae: prospecting for a new remediation biotechnology applied to saline waters. *Chem Eng J* 281:759–770. <https://doi.org/10.1016/j.cej.2015.07.013>
- Henriques B, Gonçalves G, Emami N et al (2016) Optimized graphene oxide foam with enhanced performance and high selectivity for mercury removal from water. *J Hazard Mater* 301:453–461. <https://doi.org/10.1016/j.jhazmat.2015.09.028>
- Herrero R, Lodeiro P, Rey-Castro C et al (2005) Removal of inorganic mercury from aqueous solutions by biomass of the marine macroalga *Cystoseira baccata*. *Water Res* 39:3199–3210. <https://doi.org/10.1016/j.watres.2005.05.041>
- Ho YS, McKay G (1999) Pseudo-second order model for sorption processes. *Process Biochem* 34:451–465. [https://doi.org/10.1016/S0032-9592\(98\)00112-5](https://doi.org/10.1016/S0032-9592(98)00112-5)
- Holan ZR, Volesky B (1994) Biosorption of lead and nickel by biomass of marine algae. *Biotechnol Bioeng* 43:1001–1009. <https://doi.org/10.1002/bit.260431102>
- Holan ZR, Volesky B, Prasetyo I (1993) Biosorption of cadmium by biomass of marine algae. *Biotechnol Bioeng* 41:819–825. <https://doi.org/10.1002/bit.260410808>
- Huang Y, Du JR, Zhang Y et al (2015) Removal of mercury (II) from wastewater by polyvinylamine-enhanced ultrafiltration. *Sep Purif Technol* 154:1–10. <https://doi.org/10.1016/j.seppur.2015.09.003>
- Kadukova J, Vircikova E (2005) Comparison of differences between copper bioaccumulation and biosorption. *Environ Int* 31:227–232. <https://doi.org/10.1016/j.envint.2004.09.020>
- Knutsen SH, Myslabodski DE, Larsen B, Usov AI (1994) A modified system of nomenclature for red algal galactans. *Bot Mar* 37:163–169. <https://doi.org/10.1515/botm.1994.37.2.163>
- Kumar YP, King P, Prasad VSRK (2006) Removal of copper from aqueous solution using *Ulva fasciata* sp.—a marine green algae. *J Hazard Mater* 137:367–373. <https://doi.org/10.1016/J.JHAZMAT.2006.02.010>
- Lagergren S (1898) Zur theorie der sogenannten adsorption gel Zur theorie der sogenannten adsorption gelster stoffe. *Kungliga Svenska Vetenskapsakademiens Handlingar*
- Leverett D, Thain J (2013) ICES techniques in marine environmental sciences: oyster embryo-larval bioassay (revised)

- Lopes CB, Otero M, Lin Z et al (2009) Removal of Hg²⁺ ions from aqueous solution by ETS-4 microporous titanosilicate–Kinetic and equilibrium studies. *Chem Eng J* 151:247–254
- Lopes CB, Oliveira JR, Rocha LS et al (2014) Cork stoppers as an effective sorbent for water treatment: the removal of mercury at environmentally relevant concentrations and conditions. *Environ Sci Pollut Res Int* 21:2108–2121. <https://doi.org/10.1007/s11356-013-2104-0>
- Monteiro RJR, Lopes CB, Rocha LS et al (2016) Sustainable approach for recycling seafood wastes for the removal of priority hazardous substances (Hg and Cd) from water. *J Environ Chem Eng* 4:1199–1208. <https://doi.org/10.1016/J.JECE.2016.01.021>
- Murphy V, Hughes H, McLoughlin P (2008) Comparative study of chromium biosorption by red, green and brown seaweed biomass. *Chemosphere* 70:1128–1134. <https://doi.org/10.1016/j.chemosphere.2007.08.015>
- Murphy V, Hughes H, McLoughlin P (2009) Enhancement strategies for Cu(II), Cr(III) and Cr(VI) remediation by a variety of seaweed species. *J Hazard Mater* 166:318–326. <https://doi.org/10.1016/j.jhazmat.2008.11.041>
- Nasfi FH (1995) Total mercury content of sea water on the Tunisian shore. *Fresenius Environ Bull* 4:161–168
- Plazinski W, Rudzinski W, Plazinska A (2009) Theoretical models of sorption kinetics including a surface reaction mechanism: a review. *Adv Colloid Interf Sci* 152:2–13. <https://doi.org/10.1016/J.CIS.2009.07.009>
- Rangabhashiyam S, Suganya E, Lity AV, Selvaraju N (2016) Equilibrium and kinetics studies of hexavalent chromium biosorption on a novel green macroalgae *Enteromorpha* sp. *Res Chem Intermed* 42:1275–1294. <https://doi.org/10.1007/s11164-015-2085-3>
- Rocha L, Lopes C, Borges JA et al (2013) Valuation of unmodified rice husk waste as an eco-friendly sorbent to remove mercury: a study using environmental realistic concentrations. *Water Air Soil Pollut* 224:1–18. <https://doi.org/10.1007/s11270-013-1599-9>
- Rodrigues D, Freitas AC, Pereira L et al (2015) Chemical composition of red, brown and green macroalgae from Buarcos bay in Central West Coast of Portugal. *Food Chem* 183:197–207. <https://doi.org/10.1016/j.foodchem.2015.03.057>
- Roginsky S, Zeldovich Y (1934) The catalytic oxidation of carbon monoxide on manganese dioxide. *Acta Phys Chem USSR* 1:554
- Shams Khoramabadi G, Jafari A, Hasanvand Jamshidi J (2008) Biosorption of mercury (II) from aqueous solutions by *Zygnema fanicum* Algae. *J Appl Sci* 8:2168–2172
- Stumm W, Morgan JJ (1996) *Aquatic chemistry: chemical equilibria and rates in natural waters*. Wiley, Hoboken
- Suganya T, Renganathan S (2012) Optimization and kinetic studies on algal oil extraction from marine macroalgae *Ulva lactuca*. *Bioresour Technol* 107:319–326. <https://doi.org/10.1016/j.biortech.2011.12.045>
- Sunderland EM, Krabbenhoft DP, Moreau JW et al (2009) Mercury sources, distribution, and bioavailability in the North Pacific Ocean: insights from data and models. *Glob Biogeochem Cycles* 23. <https://doi.org/10.1029/2008GB003425>
- Tavares DS, Lopes CB, Daniel-da-Silva AL et al (2016) Mercury in river, estuarine and seawaters – Is it possible to decrease realistic environmental concentrations in order to achieve environmental quality standards? *Water Res* 106:439–449. <https://doi.org/10.1016/j.watres.2016.10.031>
- Yavuz H, Denizli A, Gungunes H et al (2006) Biosorption of mercury on magnetically modified yeast cells. *Sep Purif Technol* 52:253–260. <https://doi.org/10.1016/j.seppur.2006.05.001>
- Zaib M, Athar MM, Saeed A et al (2016) Equilibrium, kinetic and thermodynamic biosorption studies of Hg(II) on red algal biomass of *Porphyridium cruentum*. *Green Chem Lett Rev* 9:179–189. <https://doi.org/10.1080/17518253.2016.1185166>

Publisher's note Springer Nature remains neutral with regard to jurisdictional claims in published maps and institutional affiliations.